JOURNAL OF GEOPHYSICAL RESEARCH, VOL. 88, NO. A9, PAGES 7065–7073, SEPTEMBER 1, 1983

In Situ Measurements of Transionospheric VLF Wave Injection

P. M. KINTNER, R. BRITTAIN, AND M. C. KELLEY

School of Electrical Engineering, Cornell University

D. L. CARPENTER

Space, Telecommunications, and Radio Science Lab, Stanford University

M. J. RYCROFT

British Antarctic Survey (NERC), Cambridge

VLF waves at 3.85 kHz from the Siple, Antarctica, transmitter were continuously measured by electric and magnetic receivers on a sounding rocket as the waves propagated through the neutral atmosphere and into the ionosphere. The change from linear to circular polarization was clearly observed along with severe attenuation of the VLF signal in the *D* region. Interferometric measurements established the index of refraction and provided an independent calibration of the rocket-borne receivers. An upper bound on the VLF power radiated is estimated to be 1.7×10^3 W during a period when the antenna was driven at 115×10^3 W. The power estimated to be entering the ionosphere is between 3 W and 12 W and depends on assumptions concerning the geometrical distribution of wave power.

INTRODUCTION

Very low frequency (VLF) radio waves are known to be amplified in the magnetosphere. Natural VLF emissions may be produced spontaneously within the magnetosphere (e.g., chorus and hiss) or may be induced by lightning strokes (whistlers). The morphology of these natural phenomena and their variation with other magnetospheric conditions suggest that under some conditions they are greatly amplified. In a series of experiments from Siple Station, Antarctica ($L = 4.2$), it was demonstrated that VLF waves artificially injected into the ionosphere and magnetosphere are frequently amplified by ~30 dB [*Helliwell and Katsufrakis*, 1974]. It was also suggested that other sources of VLF waves such as power line harmonics are also amplified [*Helliwell et al.*, 1975; *Lashinsky et al.*, 1980]. It is well known that wave amplification is associated with energetic electrons, and several authors have suggested a resonance of the VLF wave with the Doppler shifted electron gyrofrequency as a source of free energy [*Rosenberg et al.*, 1971; *Foster and Rosenberg*, 1976; *Helliwell et al.*, 1980*a*]. There is also a wave amplitude threshold above which the amplification process becomes highly nonlinear generating a variety of spectral forms [*Helliwell et al.*, 1980*b*].

Several theories based on the Doppler shift of the VLF wave frequency to the electron gyrofrequency have been introduced to explain the nonlinear amplification [*Helliwell*, 1967; *Sudan and Ott*, 1971; *Helliwell and Crystal*, 1975; *Helliwell and Inan*, 1982]. Other theoretical work concerns the perturbation of electron orbits by coherent VLF waves which produces electron precipitation [e.g., *Inan et al.*, 1978, 1982].

The need to better understand the physics of wave amplification and particle precipitation was a principle motivation for the magnetospheric physics campaign conducted at Siple during the 1980–1981 austral summer. The campaign included active experiments by the VLF transmitter at Siple, and measurements made on the ground and in balloons at Siple and its magnetic conjugate station, Roberval, Canada, plus measurements from sounding rockets at Siple. A summary of the campaign is given by *Matthews* [1981]. This and the companion paper [*Brittain et al.*, this issue] are the first full reports from that campaign.

To further develop and apply the theories of wave-particle interactions, it is necessary to know the boundary conditions such as the amplitude of the injected VLF wave. Hence, one goal of the 1980–1981 Siple campaign, and in particular the sounding rocket program was to measure the efficiency of the Siple VLF transmitter and antenna and the amplitude of the signal injected into the lower ionosphere. In this paper we report VLF wave measurements from a sounding rocket launched above the Siple VLF transmitter.

Three Nike-Tomahawk sounding rockets containing VLF wave receivers and particle detectors were launched during December of 1980 and January of 1981. The three rockets (18.203, 18.204, and 18.205) were all launched during periods of magnetospheric amplification of Siple transmissions but in different natural VLF conditions. The rocket to be discussed in this paper (18.205) was launched at 1822:18.2 UT on January 10, 1981 (~1322 MLT) to an altitude of 195 km, and it traveled 290 km to the north along a magnetic meridian. The solar elevation during the flight was approximately 35°. The 3-hour *Kp* index during the flight was 4− although the sum for the previous 24 hours was only 10+. There was little natural VLF activity during the flight. Electron precipitation was $\lesssim 10^{-3}$ erg cm^{-2} s^{-1} between 0.1 and 300 keV as seen at the rocket (D. L. Matthews, private communication, 1982). No riometer absorption was present.

During the upleg the rocket trajectory was nearly parallel to the magnetic field line intersecting Siple. To take advantage of this unusual geometry, a continuous signal at 3.85 kHz was transmitted for the first 100 of the flight of the last

Paper number 3A0809.
0148-0227/83/003A-0809$05.00

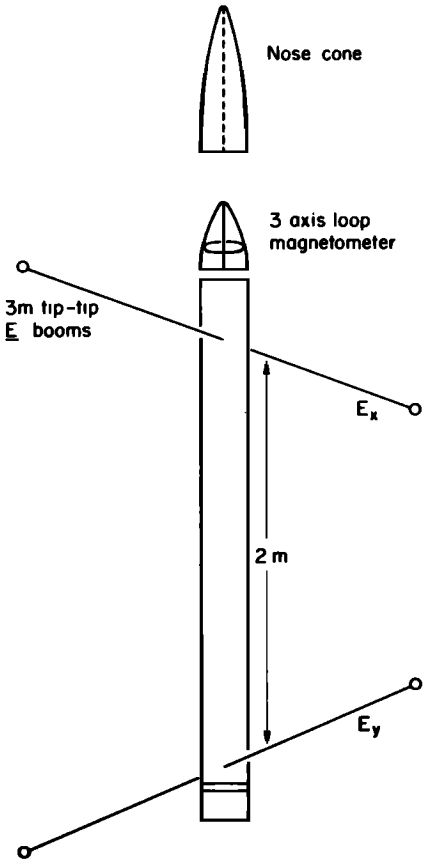

Fig. 1. Electric field and magnetic field sensors on Nike Tomahawk rockets.

rocket (18.205). Thus a continuous record of the VLF wave injection into the ionosphere was created from an altitude of 0–130 km. Shorter duration transmissions for the purpose of producing echoes occurred later in the flight and they have also been used to diagnose the injected signal. We describe here, in detail, the entrance of the transmitted VLF wave into the ionosphere.

THE ROCKET VLF WAVE RECEIVER AND EXPERIMENT

The VLF wave experiment on board the Nike-Tomahawk sounding rockets consisted of three orthogonal ac electric field measurements, three orthogonal ac magnetic field measurements, and a digital automatic gain control (DAGC) with 12 different gain states. The ac electric field was sensed using spherical probes separated by 3 m. There were two probe pairs. The axis of each probe pair was perpendicular to the rocket spin axis and they were oriented as shown in Figure 1. The z axis was taken parallel to the rocket spin axis; the x and y axes were orthogonal to the spin axis. The separation between the two boom pairs was 2 m. The z direction ac electric field was formed on board by separately averaging the signals from the upper probe pair and the lower probe pair and then amplifying their difference. The bandpass of each electric field component covered at least 30 Hz to 8 kHz.

The ac magnetic field was sensed with three orthogonal loops located at the forward most point of the payload and geometrically aligned with the three measured components of electric field. The transfer function of the ac magnetic field receiver was not constant with respect to frequency; the bandpass extended from 800 Hz to 12 kHz with a peak gain at 4 kHz.

The DAGC system amplified all six channels of ac electric and ac magnetic signals. The DAGC operated on each channel separately by sensing if the peak to peak amplified voltage was larger (less) than a preset voltage and then decreasing (increasing) the gain by a factor of 2. Each channel has 12 possible gain steps in steps of two and the gain state of all channels was changed simultaneously. The appropriately amplified ac electric and ac magnetic signals were telemetered to the ground using subcarriers on an FM-FM link.

The trajectories of all three payloads were similar. Figure 2 illustrates the trajectory of the last flight (18.205) during which the Siple transmitter broadcast a continuous wave signal at 3.85 kHz for the first 100 s of flight. The major events during the upleg were (1) the nose cone tip eject at 65 km altitude which exposed the magnetometer loops directly to the Siple signal, (2) the electric field boom deployment which was completed at 88 km, (3) and the transmitter turnoff at 130 km altitude. Hence the magnetic sensor was operating within the neutral atmosphere and during the transition through the lower ionosphere while the electric field receiver was not fully operational until entering the lower strata of the ionosphere.

Of special interest is the relation of the earth's magnetic field to the trajectory. Since the rocket was launched north along the magnetic meridian, the rocket trajectory and rocket spin axis were nearly parallel to the magnetic field (dip angle 23°) for the duration of the continuous transmission. Hence we will assume that the received wave vector was nearly parallel to the magnetic field and to the rocket spin axis. We would expect the transmitted wave vector to become more vertical upon entering the refracting ionosphere. However, our measurements of the vector ac magnetic field indicated that the transmitted wave vector was within 20° of being parallel to the earth's magnetic field and the rocket spin axis until transmitter turnoff. An angle of 20°

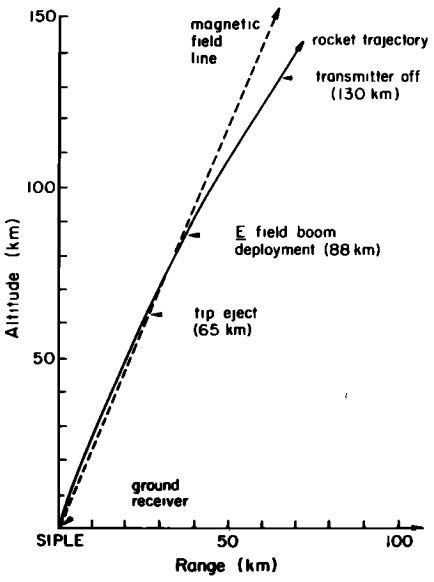

Fig. 2. Upleg trajectory and major events for Nike Tomahawk rocket 18.205.

is a sufficient approximation of parallel propagation for the calculations that follow.

ANALYSIS OF THE VLF WAVE DATA

The data were analyzed by first digitizing all of the analog wave forms at 20 kHz with 10-bit accuracy. The analysis of the data in the frequency domain was then conducted digitally using standard discrete Fourier transform algorithms (such as the fast Fourier transform). An example of the ac magnetic field data in the frequency domain is shown in Figure 3. In this case, the power spectral density calculated using a discrete Fourier transform is plotted as a function of frequency. The nonlinear frequency response of the magnetometer has been removed by multiplying by the reciprocal of the transfer function at each frequency and this is responsible for the increase in noise below 2 kHz. We have truncated the signal below 1 kHz because the gain approaches zero for smaller frequencies resulting in a large effective noise spectrum. Clearly present is the Siple transmitter signal at 3.85 kHz whose power is 10^3 larger than the background noise.

Since the Siple transmitter broadcasted a continuous tone for the first 100 seconds of the rocket flight, it is possible to study the VLF wave entry into the ionosphere. A record of the x axis VLF magnetometer signal is shown in Figure 4 as the rocket entered the ionosphere. The figure illustrates the power received between 3.5 kHz and 4 kHz as a function of time; the power was almost entirely produced by the Siple transmission. During this time period the rocket was initially spinning at 6 Hz but despun to 3 Hz as the electric field booms were deployed. The transmitted Siple signal was linearly polarized in the neutral atmosphere. Consequently, at low altitudes (below 75 km) the magnetometer signal was modulated at twice the spin frequency of the rocket. As the rocket entered the D region, about 80 km, two changes occurred. First, the spin modulation amplitude decreased as the transmitted signal became circularly polarized and, second, the overall signal amplitude decreased as collisional effects became important. As the rocket continued to rise in altitude, the spin modulation disappeared indicating that the Siple signal was completely circularly polarized; then the magnetic field amplitude increased. This latter effect is attributed to an increase in the index of refraction ($n = cB/E$), and, although the magnetic field above 90 km returned to its value at lower altitudes, the Poynting vector was only a small fraction of its earlier value.

The Poynting vector is defined by

$$S = \tfrac{1}{2}\langle \mathrm{Re}\,(E_0 \times H_0^*)\rangle \qquad (1)$$

where the brackets indicate a time average. Hence if both the wave electric field E_0 and the wave magnetic field ($B_0 = \mu_0 H_0$) are known, the Poynting vector may be calculated without any other knowledge of the plasma parameters. At lower altitudes, within the neutral atmosphere, only ac magnetic field measurements were obtained and we determine S by assuming that the index of refraction was unity ($S = \frac{1}{2}(\mu_0/\epsilon_0)^{1/2}H^2$). We show later in this paper that our assumption of $n = 1$ is valid. We must also assume that the rocket is no longer within the near field zone of the antenna. This assumption is correct if $kd \gg 1$, where k is the wave number and d is the distance from the antenna. At 60 km altitude, kd was 4.8 and increased linearly with altitude.

Several values of the Poynting vector just below and inside the ionosphere are tabulated in Table 1. Within the ionosphere the Poynting vector was estimated from a single component of ac magnetic field, a single component of ac electric field, and the following two assumptions; the wave was circularly polarized and the wave vector was parallel to the spin axis. Table 1 shows that the Poynting vector decreased by almost 2 orders of magnitude as the transmitted signal propagated from 68 km altitude to 129 km altitude. The attenuation of the signal was due to both reflection and absorption produced by electron-neutral collisions. An application of the full wave model to these processes will be the subject of later papers.

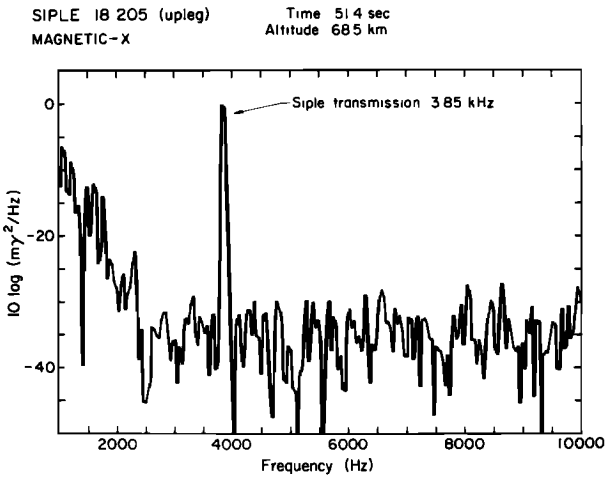

Fig. 3. Power spectrum from VLF magnetic field receiver showing the Siple transmission at 3.85 kHz.

A crude estimate of the relative importance of reflection versus absorption may be obtained from *Helliwell*'s [1965] arguments. The net power loss between 68.5 km altitude and 95.6 km altitude was observed to be about 17 dB. From this the polarization loss of 3 dB and a spreading factor loss of 3 dB may be removed to yield 11 dB. Using Helliwell's estimates of absorption in the daytime lower ionosphere, we obtain a loss of 8 dB. Consequently, reflection should account for about 3 dB of the observed decrease in the Poynting vector.

After transmitter turnoff, the two-hop whistler mode echo of the CW signal continued for about 5 s; this had a magnetic component 14 dB smaller than the upgoing transmission. The two-hop echo had power not only at the transmitter frequency but also in a narrow band extending up to 70 Hz above the transmitter frequency. Doppler effects due to sounding rocket motion can only account for about a 6-Hz frequency shift. Hence we believe the power at the additional frequencies was produced by nonlinear amplification in the wave particle interaction region. At later times in the flight two-hop echo amplitudes of short transmissions were about the same as those of upgoing transmission. This suggests that during the continuous transmission, the two-hop echo amplitude was suppressed, the suppression being a result of mixing between the injected signal and the spectrally broadened echoes as reported previously by *Raghuram et al.* [1977]. In any case, the reduced amplitude of the two-hop echo substantiates an assumption made to calculate the upgoing Poynting vector: during the continuous transmission the upgoing signal was dominant.

After the continuous tone transmission ceased at 100 s,

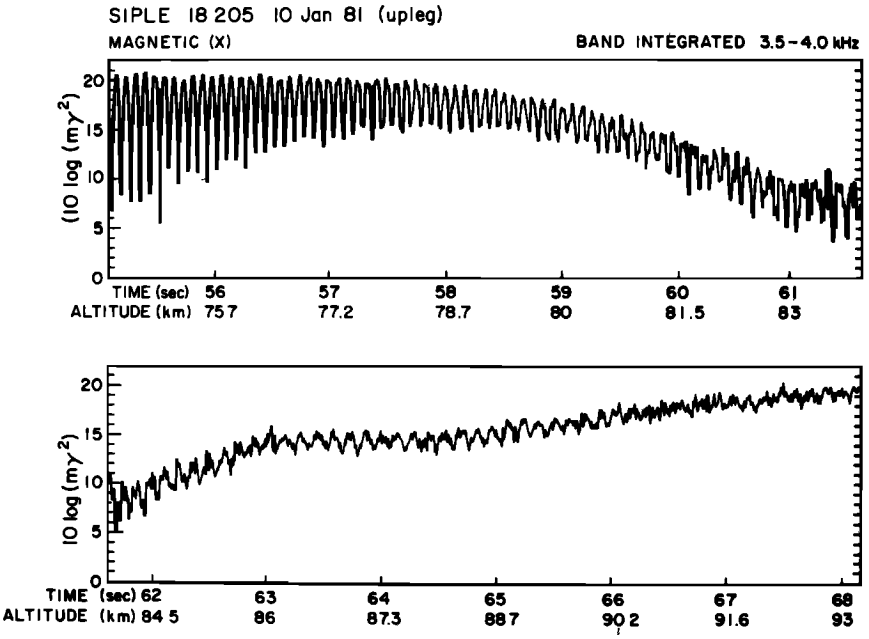

Fig. 4. Integrated Siple transmitter power received by the rocket borne VLF magnetometer over the altitude range 75–93 km. During this period the Siple transmission changes from linearly polarized to circularly polarized and is severely attenuated (see text).

there were several shorter transmissions for the purpose of stimulating echoes. Since the rocket trajectory was no longer parallel to the Siple magnetic field after 100 s, these transmissions provide information on the horizontal distribution of the transmitted signal amplitude. Figure 5 illustrates the Poynting flux as a function of horizontal range from Siple. The peak power flux within the ionosphere occurred just after the payload entry, and it continued to decrease with increasing range. The Poynting flux has decreased by an order of magnitude at a range of 150 km or approximately two wavelengths assuming a refractive index of 1. The rocket altitude (kilometers) for each measurement is indicated in parentheses. Since the electron-neutral collision frequency above 130 km is small compared to the electron gyrofrequency, we expect the changes in Poynting flux to have primarily resulted from changes in range rather than absorption. These results are consistent with studies of the distance from Siple within which injected signals were above a threshold for nonlinear magnetospheric wave growth [*Helliwell et al.*, 1980*b*] and with measurements of upgoing 12.5 kHz signals in the vicinity of an Omega transmitter [*Scarabucci*, 1969].

MEASUREMENTS OF TWO-HOP ECHO POWER

After the sounding rocket entered the ionosphere, the Siple transmitter was operated in a programed on/off mode, with 5 s on followed by 15 s off. The format consisted of two 5-s falling frequency ramps followed in sequence by a 4-s staircase and a 1-s rising ramp. Figure 6 shows the Siple signal received at the sounding rocket during a ramp and staircase. The ramp began at 1824:28 UT and after 5 s a two-hop echo appeared. The staircase pattern at 1824:48 was also followed by a two-hop echo. The two-hop echo was not a simple reproduction of the transmitted signal. A band of hiss extending 1 kHz above the transmitter frequency was also observed.

TABLE 1. Poynting Flux

Altitude, km	*Bx*, $m\gamma_{RMS}$	*Ey*, 10^{-5} V/m_{RMS}	*S*, 10^{-10} W/m^2
68.5	11	. . .	289
95.6	8.5	4.0	5.4
108.7	8.5	3.2	4.3
129.3	7.2	3.9	4.5

The power in the two-hop echo can be defined either as the power at the transmitted frequency or as the power at the transmitted frequency and within the 1-kHz band of hiss. If we just examine power within a 200-Hz band centered at the transmitter frequency, the Poynting vector of the echo was 1.9×10^{-10} W/m^2 while the upgoing signal power was 3.9×10^{-10} W/m^2. This estimate of the echo Poynting vector assumes that the echo wave vector was parallel to the rocket spin axis and the terrestrial magnetic field. We will show that this assumption is not correct; hence the echo Poynting vector is underestimated. We believe that at most the power has been underestimated by a factor of $2^{1/2}$. Examination of the total power at the transmitted frequency and within the hiss band yields an echo Poynting vector of 7.7×10^{-10} W/m^2.

The wave vector direction can be estimated from $\nabla \cdot \mathbf{B} = 0$. A Fourier decomposition of the wave magnetic field yields $\mathbf{k} \cdot \mathbf{B} = 0$. Hence the wave magnetic field vector and the wave vector are perpendicular. In this case we estimate the angle made by the magnetic field vector of the wave with the rocket spin axis known to be closely parallel to the geomagnetic field. The estimate was determined from the ratio of *Bx* to *Bz* averaged over a time longer than the rocket spin period. The result for the two-hop echo at 1824:35 indicates that the hiss band and the echo at the transmitter frequency were propagating in different directions. The component of the two-hop echo at the transmitter frequency had a wave vector which made an angle of 35° with respect to the geomagnetic field. The component of the two-hop echo

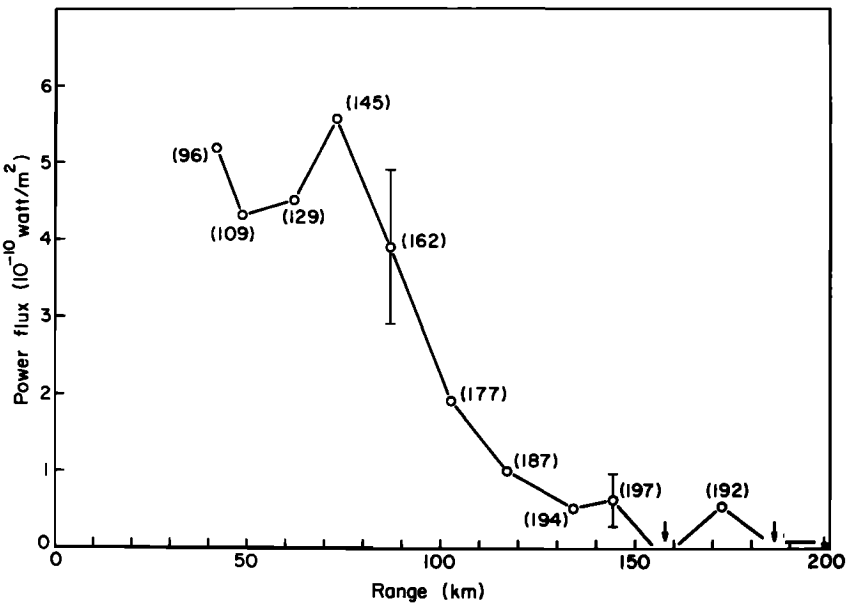

Fig. 5. VLF power from Siple transmitter received at rocket as a function of horizontal range from Siple. The numbers in parentheses are the altitudes in kilometers of each measurement.

associated with the hiss band above the transmitter frequency had a wave vector which made an angle of nearly 90° with respect to the geomagnetic field. The reader is cautioned that in an anisotropic plasma the phase velocity and group velocity are usually not parallel. In fact, for this case the 90° wave vector associated with the hiss band corresponds to a group velocity parallel to the geomagnetic field while the 35° wave vector corresponds to a group velocity about 12° from the geomagnetic field [*Helliwell*, 1965, Figure 3.8]. The analysis of wave vector direction is greatly complicated by the possibility of reflections from the lower ionosphere. In a companion paper [*Brittain et al.*, this issue], we show that reflections were likely. Hence the absolute value of the wave vector direction may be suspect. Nevertheless, it is clear that the two components of the echo were propagating in different directions.

THE INTERFEROMETER MEASUREMENT

Thus far we have discussed the amplitude of the Siple transmitter signals. The phase of these signals was also measured, hence the rocket borne VLF receiver could be employed as one end of a 'movable arm interferometer' while the other end was a ground-based VLF receiver at Siple. The total phase shift difference between the ground-based VLF receiver and the rocket VLF receiver was

$$\delta\phi = \phi_G - \phi_R = \omega t - \omega' t + \int_0^t \mathbf{k} \cdot \frac{d\mathbf{x}}{dt}\, dt + \frac{\omega|x|}{c} \qquad (2)$$

where

ω transmitter frequency;
$\omega' = \omega \pm \omega_{spin}$ received signal frequency at the rocket;
ω_{spin} rocket spin frequency;
$\mathbf{x}$ slant range to the rocket;
$\mathbf{k}$ wave vector.

Taking the derivative of (2) with respect to time yields

$$\frac{d\delta\phi}{dt} = \pm\omega_{spin} + \mathbf{k} \cdot \mathbf{v}_r + \frac{\omega}{c}|v_r| \qquad (3)$$

where $\mathbf{V}_r = d\mathbf{x}/dt$ is the rocket velocity. In estimating the left-hand side of equation (3) we measured changes of $\Delta(\delta\phi)$ in a time Δt, which yields

$$\Delta\delta\phi = \pm\omega_{spin}\,\Delta t + \mathbf{k} \cdot \mathbf{v}_r \Delta t + \frac{\omega}{c}|v_r|\Delta t \qquad (4)$$

The first term on the right-hand side of (4) is about an order of magnitude larger than the second term, which in turn is an order of magnitude larger than the third term. Since $\Delta\delta\phi$ is the measured quantity while $\mathbf{k} \cdot \mathbf{v}_r$ contains the desired physical information, it appears that ω_{spin} must be precisely calculated and removed from equation (4). However, there is a more efficient and accurate method of removing the ω_{spin} contribution to equation (4). Without loss of generality we may assert that $\delta\phi$ be a modulo 2π function. We may then take Δt to be exactly one rocket spin period, which implies that $\pm\omega_{spin}\Delta t = \pm 2\pi$. Hence the additive factor $\pm 2\pi$ may be removed from the modulo 2π function $\Delta\delta\phi$ to yield

$$\frac{\Delta\delta\phi}{\Delta t} = \mathbf{k} \cdot \mathbf{v}_r + \frac{\omega}{c}|v_r| \qquad (5)$$

The sampling of $\delta\phi$ at intervals of exactly one spin period was performed by using pulses from a solar sensor on board the rocket as a strobe. This method is accurate to better than one part in 10^3. Equation (5) may now be solved for the index of refraction ($n = ck/\omega$).

$$n = \frac{1}{\cos\theta}\left[\frac{c}{\omega v_r}\frac{\Delta\delta\phi}{\Delta t} - 1\right] \qquad (6)$$

where θ is the angle between the rocket velocity and the wave vector. We have estimated θ to be less than 20° from the ratio of the z and x magnetic fields, and we will assume that $\mathbf{k}$ and $\mathbf{V}_r$ are parallel in the calculations that follow.

The phase shift between the rocket and ground-based receiver is shown in Figure 7 on a modulo 2π scale. The digitization record began at 32 s and there was a steady but noisy change in phase until 47 s when the nose cone was ejected and the received signal amplitude greatly increased.

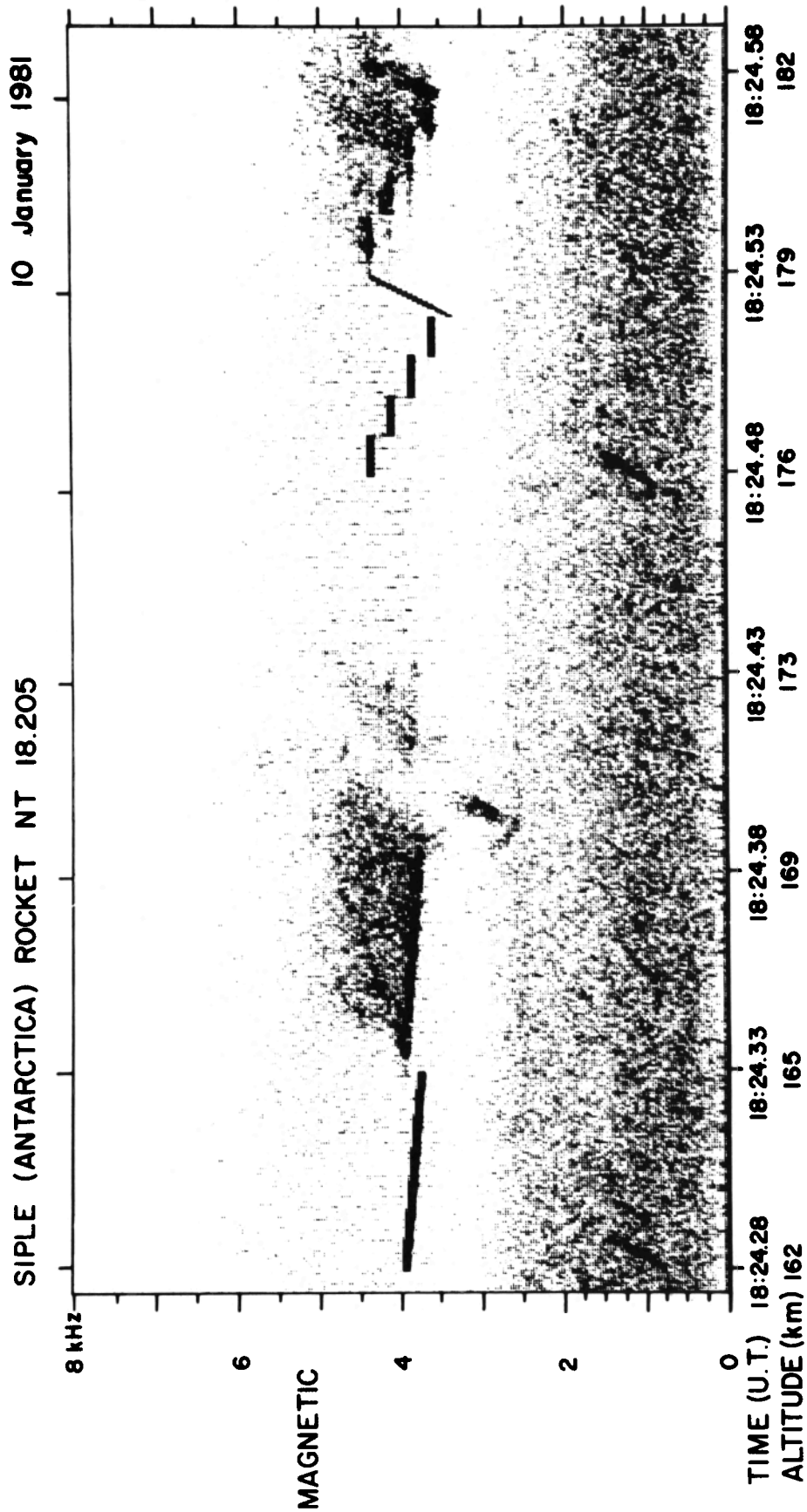

Fig. 6. Upgoing Siple transmissions followed by their two-hop echoes measured by the rocket-borne magnetic receiver. The first signal, a clearly marked descending ramp, was the upgoing transmission and was followed by another slowly descending ramp with additional spectral power above the ramp frequency. The latter emission was the two-hop echo.

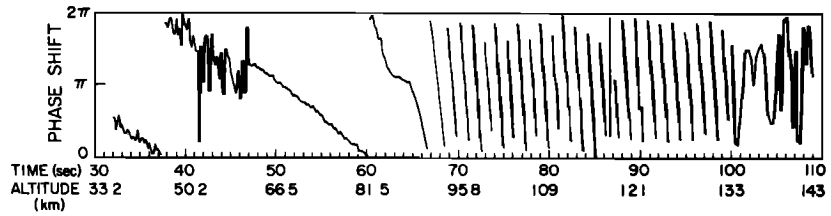

Fig. 7. The modulo 2π phase of the Siple transmission received at the rocket relative to a ground based receiver.

Between 60 s and 67 s, the wave entered the ionosphere and the phase changed irregularly. The wave behavior in this altitude range was quite complex. Both reflection and attenuation of the transmitted signal occurred as well as a change from linear to right-hand circular polarization (by removal of the left-hand polarized component). A description of the physical processes in this altitude range is beyond the scope of this paper and will be considered in later publications. Between 67 s and 100 s the phase increased smoothly but rapidly as expected for a whistler mode wave propagating in a magnetized plasma. The apparent disruption of phase at 87 s was produced by a natural whistler and, after the signal was turned off at 100 s, only random phase shifts were observed. Every $2\pi(1 + 1/n) \approx 2\pi$ repetition of the phase corresponded to the rocket traveling one wavelength, about 1.6 km in the ionosphere. This technique is similar to Doppler shift measurements made elsewhere [*Cartwright*, 1964; *Kimura et al.*, 1973; *Holtet*, 1973].

The index of refraction produced using equation (6) and by taking the derivative of Figure 7 is shown in Figure 8 for the time period of 50–100 s. At 50 s (66.5 km altitude) the rocket was well within the neutral atmosphere and the index of refraction was about 1. Between 80 km and 90 km altitude, the calculated index of refraction changed in a complex fashion and it may be incorrect. In addition to absorption of the right hand mode and collisional damping there was probably a reflected signal. Hence the derivative of phase path between 80 km and 90 km is not related to the index of refraction in a simple way. Above 90 km the index of refraction grows rapidly to an approximate value of $n = 40$ for the remainder of the continuous transmission.

The index of refraction for a whistler wave which is propagating parallel to the magnetic field is given by $n = cB/E$. Since the magnetic and electric fields were measured by the rocket VLF receiver, another measurement of the index of refraction is obtained which is independent of the phase method. The consequence of these methods being independent is a calibration of the electric and magnetic receivers in situ or, more precisely, a calibration of the ratio of the magnetic field to the electric field. Since there is no separate calibration of VLF receivers in space, this measurement is an important test of the sensor coupling to the plasma.

Several times have been chosen to make the comparison and they are plotted in Figure 8. The electric and magnetic field ratios yield an index of refraction between 50 and 60, up to 50% larger than the phase path calculation. The ratio cB/E was determined using the measured Bx and Ey components which, like the phase path calculation, assumes that the wave vector was parallel to the payload spin axis. Since both methods depend on the wave vector direction we estimate that off parallel propagation could only account for a 10% discrepancy. Although any combination of Bx overestimate and/or Ey underestimate could be responsible for the observed index of refraction, the most straightforward explanation involves a capacitive loading of the electric field signal. We have assumed a resistive contact to the plasma and, since the instrumental input resistance was much greater than the resistance between the spherical electrode and the plasma, no loading was expected. However, the input capacity is comparable to the sphere free space capacity and could play a role in the absolute calibration. Regardless of the source of the systematic error, in the worst case the Poynting vector is in error by at most 50%.

Discussion and Conclusions

The sounding rocket VLF receiver results provide a continuous measurement of the signal from the Siple trans-

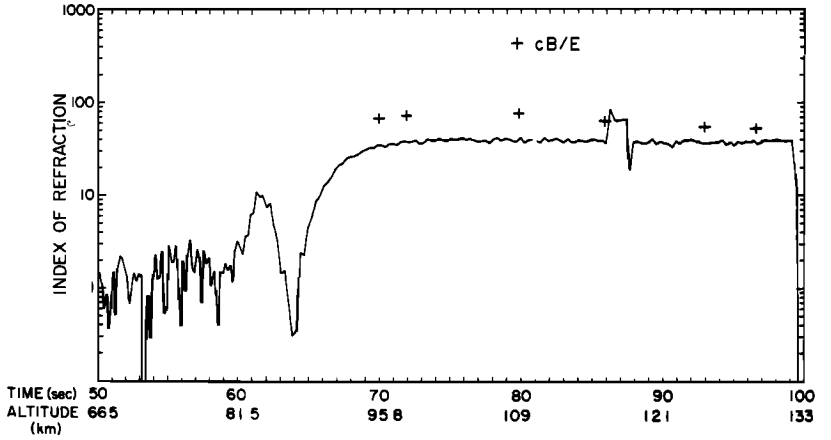

Fig. 8. The index of refraction calculated from the derivative of the phase shift in Figure 7 (see text). The crosses were obtained from the ratio of magnetic field to electric field measurements.

mitter through the neutral atmosphere and into the ionosphere. Although these electric field and magnetic field measurements are made in only two dimensions (the vertical direction and one horizontal direction) we may still make estimates of the total radiated power and the total power which entered the ionosphere.

Typical Poynting vector values are given in Table 1 and Figure 5. The transmitted Poynting vector was small compared to typical values for natural emissions. For example, on flight 18.204 the Poynting vector from natural emissions (chorus) reached values of 3×10^{-8} W/m^2. The rocket results are consistent with 1973 IMP 6 measurements of Siple signal amplitudes at much higher altitudes (3–4 R_E) [*Inan et al.*, 1977*a*, *b*]. From the IMP 6 wave magnetic field amplitudes and E/B ratios reported for $L \sim 4$ and $-20°$ latitude just inside the plasmasphere, we calculate a Poynting vector of 1.1×10^{-12} W/m^2. An equivalent number for the rocket experiment is obtained by projecting the measured value of the Poynting vector at 130 km to the IMP 6 altitude, assuming confinement of the waves within a field-aligned duct. This projection leads to a value of 7.5×10^{-12} W/m^2. To compensate for differences in radiated power between the two experiments, we multiply this number by a factor of 2.3 to allow for both small differences in power delivered to the antenna, 115 kW in 1981 in comparison to 105 kW in 1973, and a larger difference in the frequency-dependent antenna efficiency, ~0.6% in 1981 at 3.85 kHz and ~1.5% in 1973 at 5.62 kHz. The result is 17.1×10^{-12} W/m^2, which is ~12 dB above the IMP 6 values. The difference can be accounted for by a ~20 dB waveguide loss between Siple and the IMP 6 field lines, located near Halley about 1600 km to the east (Halley measurements of Siple field strengths support this estimate; J. P. Mathews, personal communication, 1979). The effect of this loss is then reduced by roughly 7 dB to account for nighttime (1973) as opposed to daytime (1981) conditions on wave absorption in the ionosphere. The agreement in amplitude of the two data sets suggests that in the case of the IMP 6 data, significant amplification had not taken place before the Siple signals reached the IMP 6 location, 20° south of the equator and in the hemisphere of the transmitter.

We may estimate an upper bound on the efficiency of the transmitter and antenna by assuming an isotropic radiation pattern. Then for a Poynting vector of 2.89×10^{-8} W/m^2 at 68 km altitude, the total radiated power over 4 steradians was 1.68×10^3 W compared to the 115×10^3 W output power from the transmitter. Hence an upper bound on the transmitter and antenna efficiency is ~1.5%. This is in good agreement with estimates by *Raghuram et al.* [1974] of 1% near 4 kHz.

An estimate of the total power injected into the ionosphere may be deduced from Figure 5. If we assume that injected wave vectors are nearly parallel to the earth's magnetic field and that they fill a cylindrical volume of 50–100 km in radius with a Poynting vector of 4×10^{-10} W/m^2 then the total injected power is between 3 W and 12 W. During darkness we expect absorption in the D layer at 3.85 kHz to decrease by about 7 dB at Siple's latitude [*Helliwell*, 1965] which implies that an upper bound on the corresponding injected power in winter would be 60 W. Small as it appears, this injection of coherent wave power is sufficient to produce amplified echoes and trigger further emissions.

Acknowledgments. This sounding rocket campaign was conducted in a particularly harsh environment and its success is a tribute to the members of the National Science Foundation, NASA/GSFC sounding rocket branch, Thiokol Corporation, University of New Mexico Physical Sciences Laboratory, Stanford University, and ITT Antarctic Services. We would particularly like to thank the project scientist David Matthews and John Katsufrakis, Gary Cooper, George Alford, and David Barnett. For assistance with transmitter operations we thank Evans Paschal and William Trabucco. Additional support was provided by M. Dermedziew and John Billey. This research was supported at Cornell by NSF grant DPP-80-23968 and at Stanford by NSF grant DPP80-22282 and DPP80-22540. The construction of the VLF magnetometers was funded by the British Science Research Council (now Science and Engineering Research Council) by grant SGD 01014.

The Editor thanks J. A. Holtet and T. L. Crystal for their assistance in evaluating this paper.

REFERENCES

Brittain, R., P. M. Kintner, M. C. Kelley, J. C. Siren, and D. L. Carpenter, Standing wave patterns in VLF hiss, *J. Geophys. Res.*, this issue.

Cartwright, D. G., A 10-kilocycle per second Doppler observation of the intermediate layer of the nighttime ionosphere, *J. Geophys. Res.*, *69*, 4031, 1964.

Foster, J. C., and T. J. Rosenberg, Electron precipitation and VLF emissions associated with cyclotron resonance interactions near the plasmapause, *J. Geophys. Res.*, *81*, 2183, 1976.

Helliwell, R. A., *Whistlers and Related Ionospheric Phenomena*, Stanford University Press, Stanford, Calif., 1965.

Helliwell, R. A., A theory of discrete VLF emissions from the magnetosphere, *J. Geophys. Res.*, *72*, 4773, 1967.

Helliwell, R. A., and T. L. Crystal, A feedback model of cyclotron interaction between whistler mode waves and energetic electrons in the magnetosphere, *J. Geophys. Res.*, *80*, 4249, 1975.

Helliwell, R. A., and U. S. Inan, VLF wave growth and discrete emission triggering in the magnetosphere: A feedback model, *J. Geophys. Res.*, *87*, 3537, 1982.

Helliwell, R. A., and J. P. Katsufrakis, VLF wave injection into the magnetosphere from Siple Station, Antarctica, *J. Geophys. Res.*, *79*, 2511, 1974.

Helliwell, R. A., J. P. Katsufrakis, T. F. Bell, and R. Raghuram, VLF line radiation in the earth's magnetosphere and its association with power system radiation, *J. Geophys. Res.*, *80*, 4249, 1975.

Helliwell, R. A., S. B. Mende, J. H. Doolittle, W. C. Armstrong, and D. L. Carpenter, Correlations between 4278 Å optical emissions and VLF wave events observed at $L = 4$ in the Antarctic, *J. Geophys. Res.*, *85*, 3376, 1980*a*.

Helliwell, R. A., D. L. Carpenter, and T. R. Miller, Power threshold for growth of VLF signals in the magnetosphere, *J. Geophys. Res.*, *85*, 3360, 1980*b*.

Holtet, J. A., Electric field measurements in the auroral *E*-region, *Geophys. Norv.*, *30* (4) 1973.

Inan, U. S., T. F. Bell, and R. R. Anderson, Cold plasma diagnostics using satellite measurements of VLF signals from ground transmitters, *J. Geophys. Res.*, *82*, 1167, 1977*a*.

Inan, U. S., T. F. Bell, D. L. Carpenter, and R. R. Anderson, Explorer 45 and IMP 6 observations in the magnetosphere of injected waves from the Siple Station VLF transmitter, *J. Geophys. Res.*, *82*, 1177, 1977*b*.

Inan, U. S., T. F. Bell, and R. A. Helliwell, Nonlinear pitch angle scattering of energetic electrons by coherent VLF waves in the magnetosphere, *J. Geophys. Res.*, *83*, 3235, 1978.

Inan, U. S., T. F. Bell, and H. C. Chang, Particle precipitation by short-duration VLF waves in the magnetosphere, *J. Geophys. Res.*, *87*, 6243, 1982.

Kimura, I., T. Tomimoto, and K. Hiraishi, Measurements of wave normal direction of whistler mode signals in the ionosphere by means of the rocket Doppler technique, *Planet Space Sci.*, *21*, 671, 1973.

Lashinsky, H., T. J. Rosenberg, and D. L. Detrick, Power line radiation: Possible evidence of vanderPol oscillations in the magnetosphere, *Geophys. Res. Lett.*, *7*, 837, 1980.

Matthews, D. L., Siple station magnetospheric physics campaign, *Antarct. J. U.S.*, *16*(5), 202–203, 1981.

Raghuram, R., R. L. Smith, and T. F. Bell, VLF antarctic antenna impedance and efficiency, *IEEE Trans. Antennas Propag.*, *AP-22*, 334, 1974.

Raghuram, R., T. F. Bell, R. A. Helliwell, and J. P. Katsufrakis, Echo-induced suppression of coherent VLF transmitter signals in the magnetosphere, *J. Geophys. Res.*, *82*, 2787, 1977.

Rosenberg, T. J., R. A. Helliwell, and J. P. Katsufrakis, Electron precipitation associated with discrete very low frequency emissions, *J. Geophys. Res.*, *76*, 8445, 1971.

Scarabucci, R. R., Interpretation of VLF signals observed on the OGO-4 satellite, *Tech. Rep. 3418-2*, Radiosci. Lab., Stanford Univ., Stanford, Calif., 1969.

Sudan, R. N., and E. Ott, Theory of triggered VLF emissions, *J. Geophys. Res.*, *76*, 4463, 1971.

R. Brittain, M. C. Kelley, and P. M. Kintner, School of Electrical Engineering, Cornell University, Ithaca, NY 14853.

D. L. Carpenter, Space, Telecommunications, and Radio Science Lab, Stanford University, Stanford, CA 94305.

M. J. Rycroft, British Antarctic Survey (NERC), Cambridge CB30ET, England.

(Received February 2, 1983;
revised May 16, 1983;
accepted May 19, 1983.)